Research Article

Intrinsic supercurrent diode effect in NbSe$_2$ nanobridge

Yiwen Zhang[1,2,#], **Jiliang Cai**[1,#], **Peng Dong**[1,2], **Jiadian He**[1,2], **Yifan Ding**[1,2], **Jinghui Wang**[1,2], **Xiang Zhou**[1,2], **Kecheng Cao**[1], **Yueshen Wu**[1,2], **Jun Li**[1,2]

[1]School of Physical Science and Technology, ShanghaiTech University, Shanghai 201210, China.
[2]ShanghaiTech Laboratory for Topological Physics, ShanghaiTech University, Shanghai 200031, China.
[#]Authors contributed equally.

Correspondence to: Prof. Jun Li, Dr. Yueshen Wu, School of Physical Science and Technology, ShanghaiTech University, 393 Middle Huaxia Road, Shanghai 201210, China. E-mail: lijun3@shanghaitech.edu.cn; wuysh@shanghaitech.edu.cn

Abstract

The significance of the superconducting diode effect (SDE) lies in its potential application as a fundamental component in the development of next-generation superconducting circuit technology. The stringent operating conditions at low temperatures have posed challenges for the conventional semiconductor diode, primarily due to its exceptionally high resistivity. In response to this limitation, various approaches have emerged to achieve the SDE, primarily involving the disruption of inversion symmetry in a two-dimensional superconductor through heterostructure fabrication. In this study, we present a direct observation of the supercurrent diode effect in a NbSe$_2$ nanobridge with a length of approximately 15 nm, created using focused helium ion beam fabrication. Nonreciprocal supercurrents were identified, reaching a peak value of approximately 380 μA for each bias polarity at $B_z^{max} = \pm 0.2$ mT. Notably, the nonreciprocal supercurrent can be toggled by altering the bias polarity. This discovery of the SDE introduces a novel avenue and mechanism through nanofabrication on a superconducting flake, offering fresh perspectives for the development of superconducting devices and potential circuits.

Keywords: Supercurrent diode effect, Ising spin-orbit interaction, nanobridge

INTRODUCTION

Nonreciprocal charge transport is a phenomenon commonly observed in semiconductors[1,2], characterized

by an electron-hole asymmetric junction that produces an asymmetric current in response to positive and negative voltages. This behavior finds extensive applications in electronic devices, including diodes, a.c./d.c. converters, optical isolators, circulators, and microwave diodes across a wide frequency spectrum[3-5]. Among these, the p-n junction, a well-established device in logic and computation, is structured by the hetero-interface of a p-type and an n-type semiconductor, resulting in an asymmetric current-voltage characteristic (IVC). However, the applicability of semiconductor junctions in quantum circuits is limited by the requirement to operate at extremely low temperatures to avoid thermal excitation. To address this challenge, a practical solution is found in the nonreciprocal supercurrent, known as the superconducting diode effect (SDE)[6]. The SDE exhibits nonreciprocity in non-dissipative superconducting current, allowing it to flow exclusively in one direction. Serving as the superconducting counterpart to a semiconducting diode, this effect has the potential to emerge as a novel non-dissipative circuit element, akin to traditional diodes. This characteristic opens up exciting possibilities in the realms of superconducting electronics[7], superconducting spintronics[8,9], and quantum information and communication technology[10,11].

In recent years, various methods have been proposed to realize the SDE. The initial discovery of SDE was reported by Ando *et al.*, who investigated a junction-free superconducting $[Nb/V/Ta]_n$ superlattice, breaking both spatial-inversion and time-reversal symmetries[12]. Subsequent research by the same team introduced another implementation of zero-field SDE using noncentrosymmetric [Nb/V/Co/V/Ta] superconducting films with 20 multilayers, demonstrating the achievability of field-free SDE through noncentrosymmetric superconductor/ferromagnet multilayers[13]. A notable advancement stems from the study of a $NbSe_2/Nb_3Br_8/NbSe_2$ Josephson junction, functioning as a field-free SDE due to the asymmetric Josephson tunneling induced by rotational symmetry breaking from Nb_3Br_8 on $NbSe_2/Nb_3Br_8$ interfaces[14]. Moreover, a supercurrent diode effect was observed in few-layer $NbSe_2$ sandwiched between BN. This observation results from the breaking of inversion symmetry caused by the presence of a few layers of $NbSe_2$[15]. The Ising superconductivity nature of the few-layer $NbSe_2$ or rotational symmetry breaking on the $NbSe_2$/BN interfaces may dominate the mechanism. It is crucial to note that prior instances of SDE were based on rotational or time-reversal symmetry breaking on the interface of a two-dimensional (2D) superconductor through other quantum materials[16-18]. This approach requires a complex technique for interface control, especially concerning electron or magnetic correlation effects on the interface. Therefore, there is a need to explore intrinsic SDE in noncentrosymmetric superconductors. Remarkably, a few-layer $NbSe_2$ has been identified as a noncentrosymmetric superconductor, possessing unique intrinsic Ising-type spin-orbit coupling (SOC) with a locked electron spin along the out-of-plane axis. Consequently, the pairing symmetry can also be disrupted to generate a nonreciprocal supercurrent[19]. Thus, the observation of intrinsic SDE in low-dimensional patterned $NbSe_2$ appears highly promising.

This study presents the observation of intrinsic SDE in a $NbSe_2$ nanobridge, created using a focused helium ion microscope. Nonreciprocal critical currents are evident without the need for artificially breaking inversion symmetry when a nonzero magnetic field is applied. Current-voltage (*I-V*) mapping illustrates the asymmetry of the critical current (I_c) concerning the magnetic field under bias polarities at $B_z = \pm 0.2$ mT. A demonstrated example of a bias-polarity-controlled superconductivity diode is provided.

MATERIALS AND METHODS

Thin $NbSe_2$ flakes are mechanically exfoliated onto a polydimethylsiloxane (PDMS) film positioned on a glass slide. Subsequently, the PDMS is stamped onto the pre-prepared electrode using a micromanipulator located beneath a microscope. The sample transfer process is conducted within a glove box filled with argon gas.

The microbridge sample was fabricated using a Laser Direct-Write Lithography System (Durham Magneto Optics Ltd) and a reactive ion beam etching system (Advance Vacuum Scandinavia AB). Figure 1A illustrates the schematic representation of the typical device. The chosen $NbSe_2$ crystal for this study has a thickness of approximately 15.4 nm [Supplementary Figure 1]. Electrical contacts and microbridge strips (1 μm wide and 4 μm long) were defined through conventional photolithography [Figure 1B]. The narrow channel serves the purpose of establishing a well-defined current direction in the constriction, indicated by the orange arrow in Figure 1A and defined as the $\hat{x}$ direction. The $\hat{z}$ axis is parallel to the stacking direction of $NbSe_2$. Subsequently, the sample was introduced into a Zeiss Orion NanoFab helium ion microscope, and a 30 kV helium beam was scanned across the microbridges to create nanobridges. A lower linear fluence may slightly influence the superconductivity of $NbSe_2$, whereas a higher linear fluence induces insulating behavior in the barrier. Within these extremes, linear fluences (600 ions/nm in this sample) were determined to selectively diminish superconductivity to a certain depth, effectively reducing the dimension of $NbSe_2$. The regions bombarded by helium ions can be identified by a scanning electron microscope (SEM) [Figure 1C and D].

The as-patterned nanobridge measures approximately 15 nm in length and 1 μm in width, depicted as a red and blue gradient area in Figure 1A. The red area signifies the region where superconductivity is disrupted, while the blue area represents $NbSe_2$ reaching the 2D limit. A schematic diagram of the helium-ion-beam milling process of $NbSe_2$ is presented in Figure 1B. During the process, He^+ implantation into the $NbSe_2$ crystal can lead to preferential sputtering of selenium atoms within the 2D transition-metal dichalcogenides (TMDs)[20], resulting in the degradation of superconductivity in the irradiated region (red area). Notably, vacancy defects caused by recoil ions serve as the primary source of superconductivity disruption. Consequently, the surface, in contrast to the underlying $NbSe_2$, can be considered nearly undamaged. As the radiation linear fluence increases, the influence depth of He ions extends, subsequently reducing the thickness of the superconducting $NbSe_2$. This process may facilitate the formation of Ising pairing in few-layer $NbSe_2$ (blue area).

Electrical transport measurements were conducted utilizing a Physical Property Measurement System (PPMS-Dynacool, Quantum Design) with the external electric meter comprising a Keithley 2400 as the current source and a Keithley 2182 as the voltage meter. The investigation of transport properties employed conventional four-terminal methods.

RESULTS AND DISCUSSION

In monolayer or few-layer $NbSe_2$, the in-plane inversion symmetry is disrupted. Consequently, the concurrent impact of the Zeeman effect and substantial intrinsic spin-orbit interactions gives rise to an electron-spin-locking phenomenon along the out-of-plane direction[19,21-23] [Figure 1E]. Ising-type superconducting pairing symmetry emerges in $NbSe_2$ due to the reverse spin splitting within the valence bands near valleys K and K'. This phenomenon gives rise to intervalley spin-momentum-locked spin-singlet Cooper pairing between two electrons, characterized by opposing momenta and antiparallel out-of-plane spins.

The directions of the inversion symmetry break ($\hat{r}$) and the current ($\hat{I}$) have been illustrated in Figure 1E. Consequently, the supercurrent diode behavior of this nanobridge can be influenced by the out-of-plane component (B_z) of the magnetic field. When the applied magnetic field (B), electric current (I), and polar axis (r) are mutually orthogonal, the critical current (I_c) magnitude depends on both B and r, leading to a magnetic chiral effect[24]. Therefore, the supercurrent diode behavior is determined by the out-of-plane component B_z.
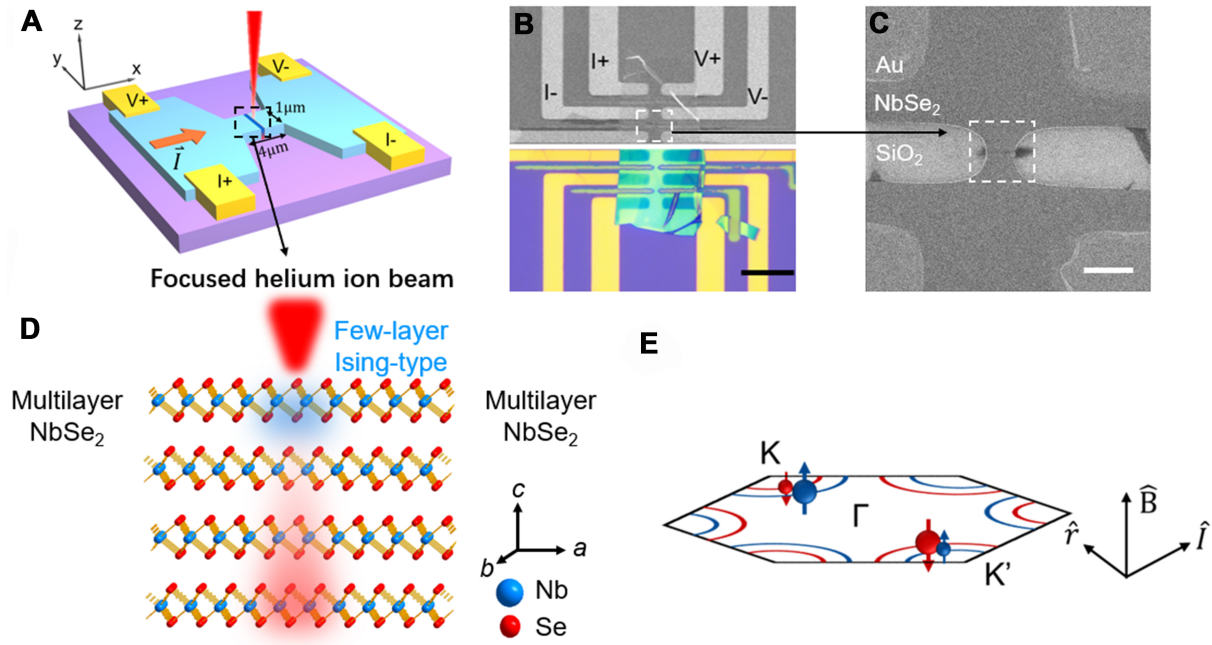
Figure 1. (A) Schematic illustration of the measurement configuration. The orange arrow indicates the supercurrent pathway, and the red laser indicates the focused helium ion beam creating a weakly coupled junction in the multilayer $NbSe_2$. The central constriction is about 1 μm wide and 15 nm long. The direction of the supercurrent is defined along the x-axis, while the z-axis is perpendicular to the crystal plane; (B) Artistic representation of the focused helium ion beam etching the multilayer $NbSe_2$. The crystal structure is that of $NbSe_2$; (C) SEM (upper) and optical (lower) image of the device. The nanobridge is made by ion beam etching, and an Ohmic contact is made by the pick-up and transfer method; scale bar, 20 μm; (D) A zoom-in image of the dashed rectangular area shown in (B). The color change reflects the change in electrical conductivity, which can be observed; (E) Illustration depicting type-I Ising superconductivity: the pairing of electrons in valleys with opposite spin splitting. $\hat{r}$ ($\hat{y}$) refers to the direction of space inversion symmetry breaking, $\hat{B}$ ($\hat{z}$) refers to the direction of time inversion symmetry breaking, and $\hat{I}$ ($\hat{x}$) refers to the current direction. SEM: Scanning electron microscope.

Figure 2 illustrates the nonreciprocal transport properties of the $NbSe_2$ nanobridge under varying irradiation linear fluences. Figure 2A-C depicts three pairs of IVCs corresponding to the magnetic fields applied along the $\hat{z}$-axis. I-V curves are recorded under $B_z = 0$ (top), $B_z = 0.7$ mT (middle), and $B_z = -0.7$ mT (bottom) for three linear fluences. All curves represent zero-to-finite (either positive or negative) bias sweep directions, mitigating potential heating effects. The orange (blue) curve denotes the current density in the nanobridge oriented toward the positive (negative) $\hat{x}$ direction. Two additional devices, fabricated with $NbSe_2$ of identical thickness, were irradiated at different linear fluences. Figure 2A and B displays the I-V curves for the devices under irradiation linear fluences of 0 and 300 ions/nm. Notably, nonreciprocal charge transport is absent in these samples. Given the intrinsic thickness of the $NbSe_2$ flake at 15.4 nm, the Ising SOC may be ineffective, and it is reasonable to assume the preservation of inversion symmetry[22]. The minimal irradiation of 300 ions/nm appears insufficient to influence the superconductivity of the nanobridge region, as evidenced by the absence of nonreciprocal transport.

As the irradiation linear fluence increases to 600 ions/nm, a robust SDE becomes evident, as depicted in the I-V curves in Figure 2C. Notably, a significant disparity exists in linear fluences between I_c^+ and $|I_c^-|$ in the critical current for the two supercurrent orientations. The sign of $\Delta = I_c^+ - |I_c^-|$ changes with the reversal of the magnetic field B_z, confirming that Δ is intrinsically determined by the magnetic field. The I-V loop further excludes the influence of thermal effects [Supplementary Figure 2]. It is essential to note that the nanobridge appears to be slightly damaged under helium ion irradiation, as evidenced by optical microscope and SEM images [Figure 1C and D]. A zoom-in image can clearly show the area of helium ion
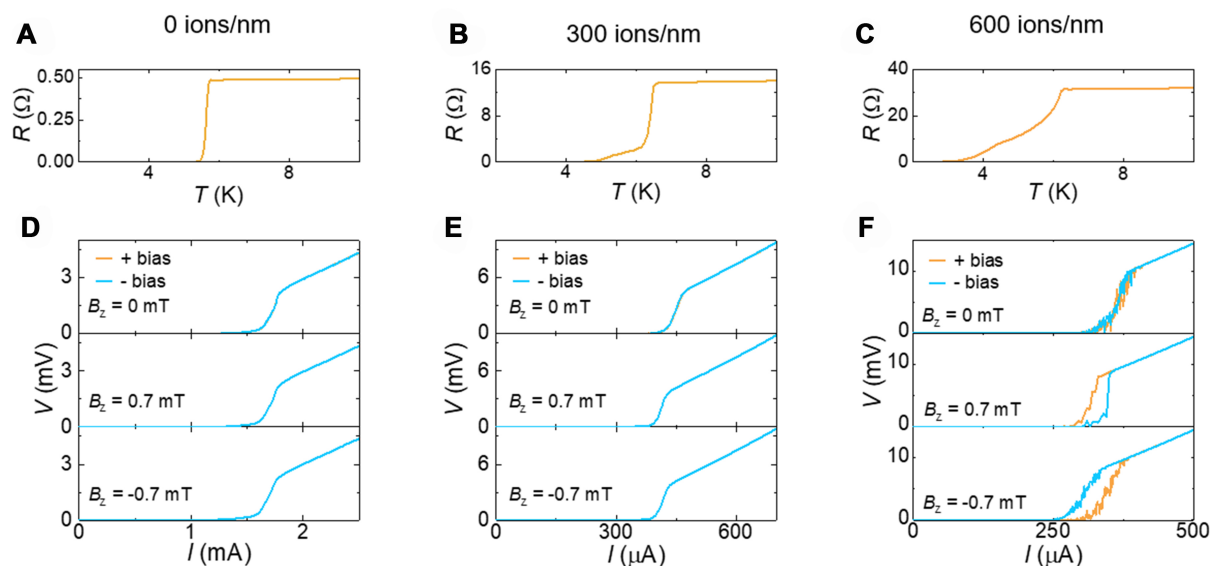
Figure 2. (A-C) Current-voltage characteristics were measured at 2 K, considering opposite bias polarities (current directions) in a 4-terminal configuration, under zero magnetic field B_z = 0 T, which is always applied parallel to the z direction. The bias sweep direction consistently proceeds from 0 to a finite bias. But for B_z = -0.7 mT. (A) and (B) Measurement for 0 and 300 ions/nm sample; (C) 600 ions/nm sample. There is a difference between two critical currents. With the orientation of the magnetic field reversed, the roles of the two bias polarities are also exchanged; (D-F) The temperature-dependent resistance under different linear fluences ranging from 0 to 600 ions/nm.

radiation framed by a dashed rectangle. We hypothesize that helium ions might influence chemical bonds or even induce doping[25,26], rather than causing a direct etching effect. Similar to the outcomes of electron beam irradiation[27], helium ion irradiation can introduce disorders into thin crystals, potentially suppressing superconductivity. Temperature dependence of resistance [Figure 2D-F] exhibits a broadened superconducting transition region with increasing linear fluences, which indicates the degradation of superconductivity in the nanobridge. Consequently, our focus shifts to the study of the sample under 600 ions/nm irradiation. The results of the other two devices (Device#4 and Device#5) have been shown in Supplementary Figures 3-5.

The *I-V* values at 2 K under various magnetic fields are presented in Figure 3A, where the color bar reflects the differential resistance (dV/dI). An enlarged view around zero field is provided in Figure 3B, revealing a distinct asymmetric behavior. The maximum of the differential resistance is defined as the critical current (I_c). The I_c values for both positive (I_c^+) and negative ($|I_c^-|$) sides are plotted under different magnetic fields [Figure 3C]. The range between the positive critical current (I_c^+) and the absolute value of the negative critical current ($|I_c^-|$) defines the supercurrent diode regime. In this regime, the current flows without dissipation in only one direction, and this direction can be chosen by altering the sign of the magnetic field. These curves clearly demonstrate that the sign of nonreciprocal components in I_c is exclusively determined by the relative orientation of the current and magnetic field. Regardless of the bias polarity, the critical current increases with the magnetic field, peaking at a nonzero field ($B_{zmax} \approx 0.2$ mT).

The substantial rise in the critical current is vital as it dismisses the possibility of the nonreciprocal supercurrent originating from Joule heating[15]. Although the origin of the supercurrent diode effect in NbSe$_2$ requires further investigation, several potential explanations can be considered. These include the interplay between Meissner currents and barriers for vortex entry[28,29], vortex flow in asymmetric pinning potentials[19], and the influence of valley-Zeeman spin-orbit interaction[15]. It is noteworthy that the observed
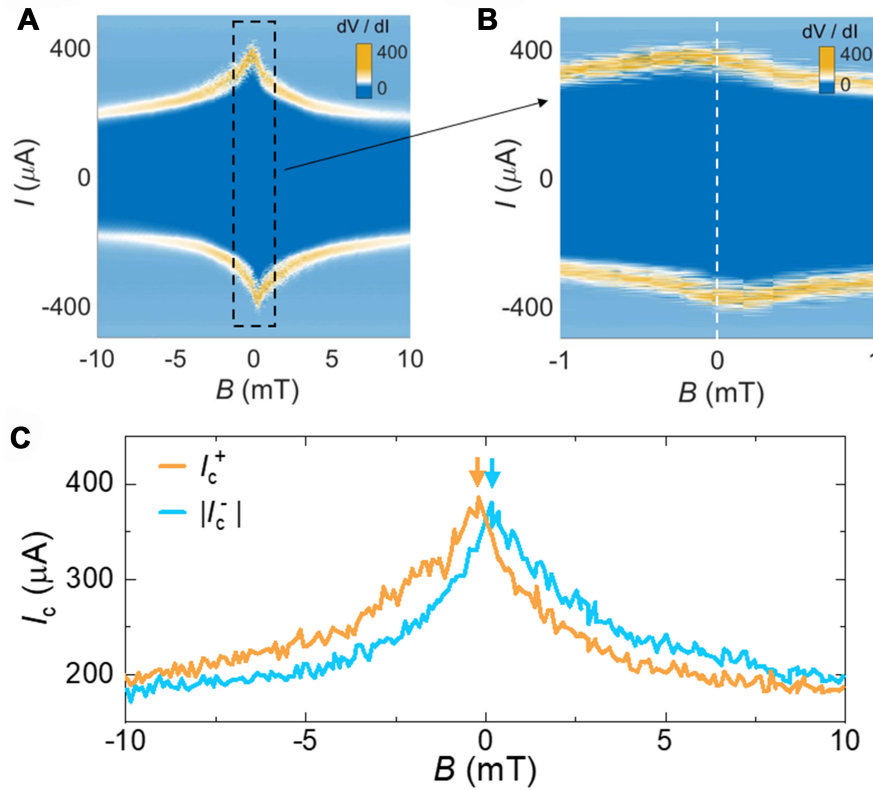
Figure 3. (A) A color map of critical current in the plane of magnetic field at 2 K, and a color bar shows the value of dV/dI. An apparent current asymmetry with respect to the magnetic field can be observed. The critical current can be extracted, as shown in (C); (B) A magnification of (A). The red dotted line marks the zero-field position; (C) Nonreciprocal critical current (I_c) as a function of B_z, with positive bias (orange) and negative bias (red), exhibiting symmetry across reflection about $B_z = 0$. The critical current peaks at a nonzero $|B_{zmax}| = 0.2$ mT, indicated by labeled orange and blue arrows.

behavior closely resembles the characteristics of NbSe$_2$ in the 2D limit[19,21,22,30,31], despite our sample having a thickness of approximately 15.4 nm. However, upon dimension reduction in the nanobridge, phenomena akin to those observed in Josephson junctions emerge [Supplementary Figure 4]. It is noteworthy that in non-uniform Josephson junctions, the dominance of Josephson vortex motion leads to an asymmetric Fraunhofer pattern[32,33]. A recent experimental study has successfully achieved SDE by introducing a non-uniform current and a single Abrikosov vortice in the junction electrodes[34]. Actually, the non-uniform penetration of helium ions can induce a non-uniform supercurrent, even when the current is uniform based on the geometry of the device [Supplementary Figure 6]. This inhomogeneity can amplify the SDE, particularly in the presence of a large critical current density, 26.7 mA·μm^{-2} in this instance.

The primary outcome of our observations indicates that the supercurrent diode effect in the NbSe$_2$ nanobridge is governed by the out-of-plane magnetic field. Based on this idea, we demonstrated bias-polarity-controlled SDE at 2 K, 0.2 mT, where the $|I_c^-|$ reaches the maximum [Figure 4]. The values of I_c^+ and $|I_c^-|$ are 345 and 380 μA, respectively. A square-wave excitation with an amplitude of 340 μA is applied [Figure 4, top panel]. The bottom panel of Figure 4 reveals that the nanobridge maintains the superconducting state with negative current (blue area) and transitions to the normal state during positive current (white area). This outcome strongly suggests that the switch between superconducting and normal conducting states is contingent on the magnetic field's sign and the current direction. Consequently, the
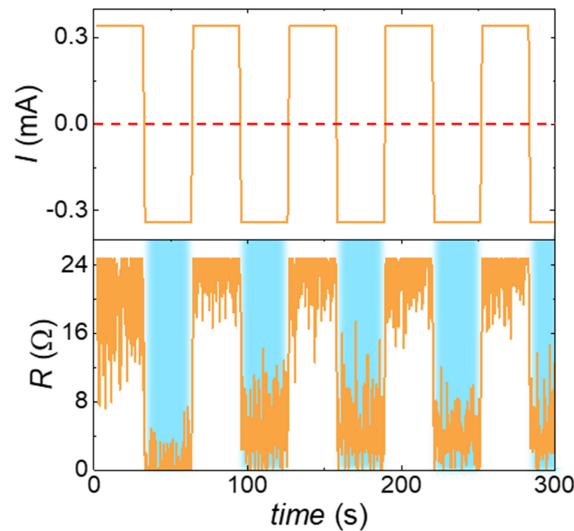
Figure 4. Controllable superconducting diode. The top panel displays the square-wave excitation applied at 2 K with an amplitude of 340 µA (between I_c^+ and $|I_c^-|$) under a magnetic field of 0.2 mT. The coincidentally measured junction voltage is presented in the bottom panel. In this depiction, the blue shaded region represents the superconducting state, where the voltage remains zero under negative current bias. Conversely, the white region signifies the normal state, with a high voltage observed during positive current bias. The red dotted line denotes the zero line.

nonreciprocity can be readily manipulated by altering the bias polarity of the applied current under a small magnetic field.

CONCLUSIONS

In conclusion, we have illustrated a supercurrent diode effect in a $NbSe_2$ nanobridge fabricated using a focused helium ion microscope. Our findings indicate that this effect is governed by the out-of-plane magnetic field, presenting a deviation from observations in Rashba superconductors. Nonreciprocal critical currents can be well turned under bias polarities at $B_{zmax} = \pm 0.2$ mT. Helium ions break the superconductivity at a certain depth and shrink the thickness of the superconductor to 2D limit. The findings suggest that the supercurrent diode effect may be linked to the inversion symmetry breaking caused by Ising SOC in a few layers of $NbSe_2$ and can be improved by heterogeneous penetration of helium ions. This insight offers a potential avenue for comprehending and optimizing the performance of the supercurrent diode effect, with implications for its application in superconducting logic and memory devices.

DECLARATIONS

Acknowledgments

Authors' contributions
Made substantial contributions to the conception and design of the study and performed data analysis and interpretation: Zhang Y

Transmission electron microscopy (TEM) and ion damage calculation: Cai J, Cao K
Writing, review and editing: Zhang Y, Wu Y, Li J
Investigation: Dong P, He J, Ding Y, Wang J, Zhou X

Availability of data and materials
Not applicable.

Conflicts of interest
All authors declared that there are no conflicts of interest.

Ethical approval and consent to participate
Not applicable.

Consent for publication
Not applicable.

REFERENCES
1. Scaff JH, Ohl RS. Development of silicon crystal rectifiers for microwave radar receivers. *Bell Syst Tech J* 1947;26:1-30. DOI
2. Shockley W. The theory of *p-n* junctions in semiconductors and *p-n* junction transistors. *Bell Syst Tech J* 1949;28:435-89. DOI
3. Tokura Y, Nagaosa N. Nonreciprocal responses from non-centrosymmetric quantum materials. *Nat Commun* 2018;9:3740. DOI PubMed PMC
4. Saito M, Ishikawa K, Taniguchi K, Arima T. Magnetic control of crystal chirality and the existence of a large magneto-optical dichroism effect in CuB_2O_4. *Phys Rev Lett* 2008;101:117402. DOI PubMed
5. Okamura Y, Kagawa F, Mochizuki M, et al. Microwave magnetoelectric effect via skyrmion resonance modes in a helimagnetic multiferroic. *Nat Commun* 2013;4:2391. DOI
6. Nadeem M, Fuhrer MS, Wang X. The superconducting diode effect. *Nat Rev Phys* 2023;5:558-77. DOI
7. Braginski AI. Superconductor electronics: status and outlook. *J Supercond Nov Magn* 2019;32:23-44. DOI
8. Linder J, Robinson JWA. Superconducting spintronics. *Nature Phys* 2015;11:307-15. DOI
9. Cai R, Žutić I, Han W. Superconductor/ferromagnet heterostructures: a platform for superconducting spintronics and quantum computation. *Adv Quantum Tech* 2023;6:2200080. DOI
10. Wendin G. Quantum information processing with superconducting circuits: a review. *Rep Prog Phys* 2017;80:106001. DOI PubMed
11. Liu X, Hersam MC. 2D materials for quantum information science. *Nat Rev Mater* 2019;4:669-84. DOI
12. Ando F, Miyasaka Y, Li T, et al. Observation of superconducting diode effect. *Nature* 2020;584:373-6. DOI
13. Narita H, Ishizuka J, Kawarazaki R, et al. Field-free superconducting diode effect in noncentrosymmetric superconductor/ferromagnet multilayers. *Nat Nanotechnol* 2022;17:823-8. DOI
14. Wu H, Wang Y, Xu Y, et al. The field-free Josephson diode in a van der Waals heterostructure. *Nature* 2022;604:653-6. DOI
15. Bauriedl L, Bäuml C, Fuchs L, et al. Supercurrent diode effect and magnetochiral anisotropy in few-layer $NbSe_2$. *Nat Commun* 2022;13:4266. DOI PubMed PMC
16. de Vries FK, Portolés E, Zheng G, et al. Gate-defined Josephson junctions in magic-angle twisted bilayer graphene. *Nat Nanotechnol* 2021;16:760-3. DOI
17. Jeon KR, Kim JK, Yoon J, et al. Zero-field polarity-reversible Josephson supercurrent diodes enabled by a proximity-magnetized Pt barrier. *Nat Mater* 2022;21:1008-13. DOI

18.　Anwar MS, Nakamura T, Ishiguro R, et al. Spontaneous superconducting diode effect in non-magnetic $Nb/Ru/Sr_2RuO_4$ topological junctions. *Commun Phys* 2023;6:290.　DOI

19.　Zhang E, Xu X, Zou YC, et al. Nonreciprocal superconducting $NbSe_2$ antenna. *Nat Commun* 2020;11:5634.　DOI PubMed PMC

20.　Stanford MG, Pudasaini PR, Belianinov A, et al. Focused helium-ion beam irradiation effects on electrical transport properties of few-layer WSe_2: enabling nanoscale direct write homo-junctions. *Sci Rep* 2016;6:27276.　DOI PubMed PMC

21.　Xi X, Wang Z, Zhao W, et al. Ising pairing in superconducting $NbSe_2$ atomic layers. *Nature Phys* 2016;12:139-43.　DOI

22.　de la Barrera SC, Sinko MR, Gopalan DP, et al. Tuning Ising superconductivity with layer and spin-orbit coupling in two-dimensional transition-metal dichalcogenides. *Nat Commun* 2018;9:1427.　DOI

23.　Yi H, Hu LH, Wang Y, et al. Crossover from Ising- to Rashba-type superconductivity in epitaxial Bi_2Se_3/monolayer $NbSe_2$ heterostructures. *Nat Mater* 2022;21:1366-72.　DOI

24.　Edelstein VM. The Ginzburg - Landau equation for superconductors of polar symmetry. *J Phys Condens Matter* 1996;8:339.　DOI

25.　Matsui H, Nishijima G, Matsumoto A, Yamaguchi I, Manabe T, Sohma M. Nonreciprocal critical current in an obliquely ion-irradiated $YBa_2Cu_3O_7$ film. *Appl Phys Lett* 2023;122:172601.　DOI

26.　Palau A, Monton C, Rouco V, Obradors X, Puig T. Guided vortex motion in $YBa_2Cu_3O_7$ thin films with collective ratchet pinning potentials. *Phys Rev B* 2012;85:012502.　DOI

27.　Cho K, Kończykowski M, Teknowijoyo S, et al. Using controlled disorder to probe the interplay between charge order and superconductivity in $NbSe_2$. *Nat Commun* 2018;9:2796.　DOI PubMed PMC

28.　Hou Y, Nichele F, Chi H, et al. Ubiquitous superconducting diode effect in superconductor thin films. *Phys Rev Lett* 2023;131:027001.　DOI

29.　Gutfreund A, Matsuki H, Plastovets V, et al. Direct observation of a superconducting vortex diode. *Nat Commun* 2023;14:1630.　DOI PubMed PMC

30.　Sohn E, Xi X, He WY, et al. An unusual continuous paramagnetic-limited superconducting phase transition in 2D $NbSe_2$. *Nat Mater* 2018;17:504-8.　DOI

31.　Falson J, Xu Y, Liao M, et al. Type-II Ising pairing in few-layer stanene. *Science* 2020;367:1454-7.　DOI

32.　Goldman AM, Kreisman PJ. Meissner effect and vortex penetration in Josephson junctions. *Phys Rev* 1967;164:544-7.　DOI

33.　Krasnov VM, Oboznov VA, Pedersen NF. Fluxon dynamics in long Josephson junctions in the presence of a temperature gradient or spatial nonuniformity. *Phys Rev B* 1997;55:14486-98.　DOI

34.　Golod T, Krasnov VM. Demonstration of a superconducting diode-with-memory, operational at zero magnetic field with switchable nonreciprocity. *Nat Commun* 2022;13:3658.　DOI PubMed PMC